Journal of Solar Energy Research (JSER)

Journal homepage: www.jser.ut.ac.ir

Photoelectrochemical Hydrogen Generation in Coral-like TiO_2 Photoanode

Bayat[a],A., Saievar-Iranizad[a,*],E.

[a]*Department of physics, Faculty of Basic Science, Tarbiat Modares University, Tehran, Iran.*
**E-Mail: saievare@modares.ac.ir*

ARTICLE INFO

Received: 9 August 2016
Received in revised form: 10 October 2016
Accepted: 11 October 2016

Keywords:
Water splitting; Coral TiO_2; Hydrothermal, Hydrogen generation

A B S T R A C T

The coral-like TiO_2 nanoparticles were synthesized on the transparent FTO conductive substrate and their photovoltaic properties investigated under illumination. Coral-like TiO_2 photoanodes were synthesized using a hydrothermal method and annealed at 450 ˚C to obtain better crystallinity. Annealed coral-like TiO_2 show a photocurrent enhancement of ~50% compared to pristine coral-like TiO_2 without annealing using 1M Na_2SO_4 as electrolyte at potential of 0 V.

Introduction

Solar water splitting and generation of hydrogen through semiconductor photocatalysts which is as an alternative candidate to the traditional fossil energy, has become the global attention[1-4]. TiO_2 has been intensively studied as the photocatalyst to date due to its favorable band-edge positions for water splitting, high resistance to photocorrosion, excellent physical and chemical stability, nontoxicity, low-cost and abundance[5-10]. TiO_2 has three phases[11, 12] (anatase, rutile and brookite) which among them anatase and rutile phases are photocatalytically active material. The difference in the band gap between anatase and rutile is mainly due to the difference in the conduction band energy (E_c) levels. The E_c of anatase is higher than that of rutile leading to the difference in photocatalytic abilities between anatase and rutile, and band gap of rutile type is less than anatase phase[12]. Thus, rutile phase of TiO_2 is favourable for photoelectrochemical applications (see Fig 1). A common approach for improving photoelectrochemical properties of photoanodes is photo-management with introducing micro and nanometric roughness on the photoanodes surfaces.

In this research we have used rutile coral-like TiO_2 as a semiconductor photoanode because of its large surface area originating from its special shape and favorable band-

edge positions for water splitting and consequently generation of H_2. Identifying the electron transfer mechanism at interface of photoanode/electrolyte under photoirradiation could be informative to better understanding photoelectrochemical systems.

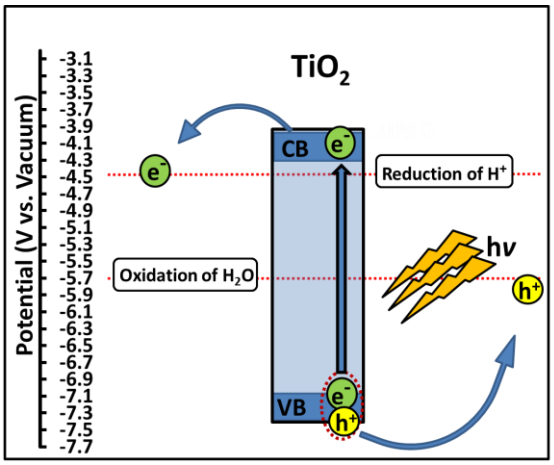

Figure 1. Generation mechanism of H_2 under illumination at TiO_2

Experimental

Coral-like TiO_2 were grown on the fluorine-doped tin oxide (FTO, F:SnO_2) using a hydrothermal method without using TiO_2 seed layer. In a typical synthesis, 12 mL of deionized water was mixed with 6 mL of concentrated hydrochloric acid to reach a total volume of 18 mL in a Teflon-lined stainless steel autoclave (75 mL volume). After addition of 1 mL of titanium (IV) isopropoxide (TTIP), the mixture was stirred under ambient conditions for 5 min. After that, the pieces of FTO substrates (F:SnO_2, 1×1.5 cm^2) were ultrasonically cleaned for 15 min in deionized water and in acetone and put into the autoclave. The hydrothermal synthesis was conducted at 160 ˚C for 15 h in an oven. After synthesing, the autoclave was cooled to room temperature naturally. The obtained samples were washed with deionized water and dried at 80 ˚C in air. Then, samples were annealed at 450 ˚C for 1 h in a furnace and naturrally cooled to room temperature.

Structural morphology of samples was studied using a scanning electron microscope (CM30 300kV). Steady state current density voltage (J-V) measurements were carried out using a VSP-300 Multichannel Potentiostat/Galvanostat (Bio-Logic Science Instruments). X-ray diffraction patterns (XRD, Co-Kα radiation source, Philips, X'Pert MPD) were studied in order to investigate the lattice structures. Raman analysis (BRUKER, Germany, SENTERRA) was used to prove the formation of rutile phase of TiO_2 photoanodes. For JV measurements, three electrode configurations was used, where the coral-like TiO_2 photoanodes were connected to the working electrode, and a saturated Ag/AgCl was used as the reference electrode and a Pt wire was connected to the counter electrode. The solution of Na_2SO_4 (1M, pH 6) was used as the electrolyte, and electrodes were illuminated using a xenon lamp and the light intensity was adjusted with a thermopile to 100 mW/cm^2.

Results & Discussion

Figure 2 shows typical top view and cross section FESEM images of the coral-like TiO_2 films grown at 160 °C for 15 h. FESEM images reveal that the entire surface of the FTO substrate is covered uniformly with coral-like TiO_2. According to this picture, coral-like TiO_2 are composed from nanorods, with an average diameter determined about 60 nm.

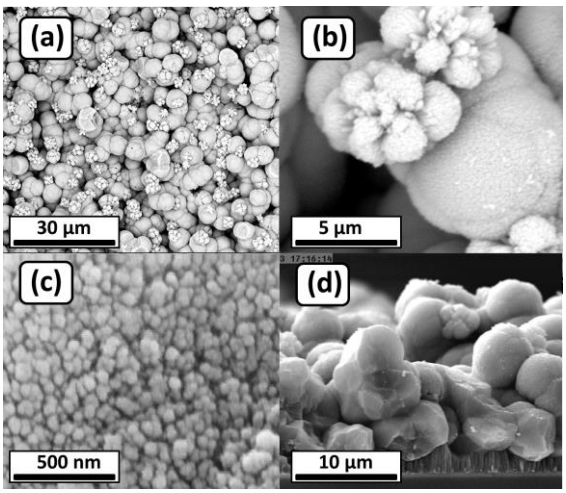

Figure 2. (a), (b) and (c) Top-view FESEM images of the coral-like TiO_2 at different scales, (d) cross section of FESEM image of the coral-like TiO_2 grown on the FTO substrate.

Figure 3 shows the XRD patterns of coral-like TiO_2 grown on the FTO substrate. The relation between the FTO substrate and rutile TiO_2 with a small lattice mismatch plays a key role in driving the nucleation and growth of the rutile coral-like TiO_2 on the FTO as substrate. According to this method, the rutile TiO_2 film deposited on FTO substrate and all diffraction peaks agree well with the tetragonal rutile phase[13, 14]. No peaks of anatase or brookite phase were detected, indicating the purity of the rutile phase. Other peaks originate from the FTO substrate.

Raman spectroscopy was employed to confirm the formation of TiO_2 rutile phase. Raman spectrum of coral-like TiO_2 is shown in Figure 4. The spectrum of coral-like

TiO_2 reveals two raman peaks at 450 and 620 cm^{-1}, which were assigned to E_g and A_{1g} modes, respectively. These peaks could be well attributed to the rutile phase of TiO_2[15, 16]. These results from Raman spectroscopy led to the conclusion that rutile coral-like TiO_2 was grown on the FTO substrate.

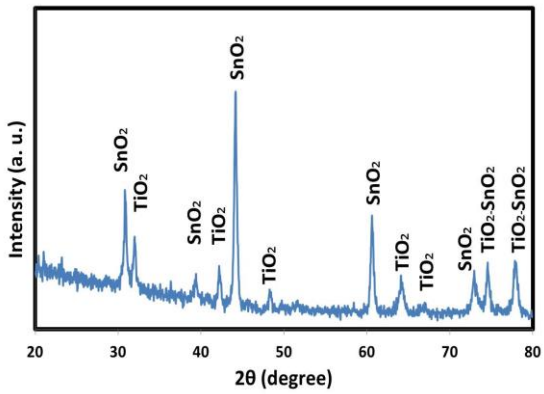

Figure 3. XRD patterns of the rutile type coral-like TiO_2 grown on the FTO substrate.

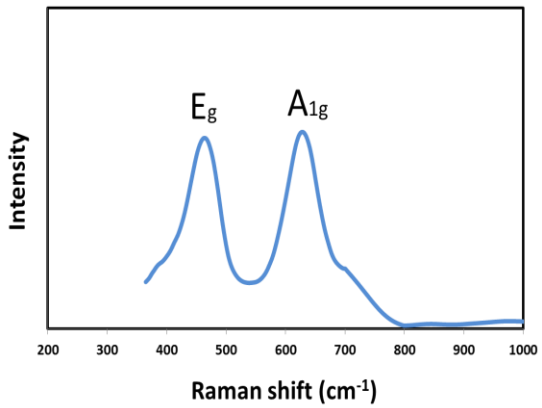

Figure 4. Raman spectrum of coral-like TiO_2.

Electron-hole generation and transmission of electrons to Pt and generation of O_2 and H_2 are schematically explained in Figure 5. According to band positions, holes at coral-like TiO_2 can be injected into the solution, while photogenerated electrons are injected into contact (charge collector) and then to the Pt as counter electrode[17, 18].

JV curves for pristine and annealed coral-like TiO_2 photoanodes are shown in Figure 6. The charge transfer kinetics is systematically faster for annealed coral-like TiO_2 sample against pristine coral-like TiO_2 as evidenced by the higher charge versus Ag/AgCl as reference.

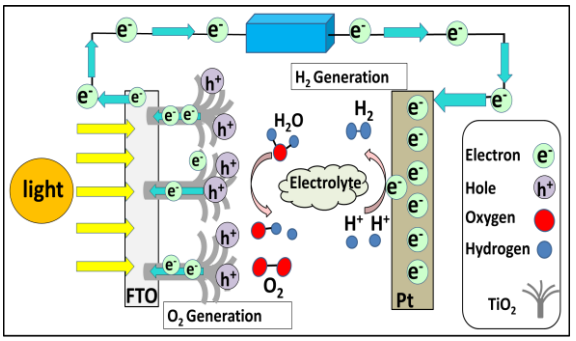

Figure 5. Schematic illustration of H_2 and O_2 generation, charge transfer mechanism at coral-like TiO_2/electrolyte interface.

Under illumination, the resulting photoinduced charge accumulation at annealed coral-like TiO_2 is believed to be the reason for the significantly increased current density. The possible mechanism of the observed photoinduced charge accumulation at annealed coral-like TiO_2 can be explained because of better crystallinity and better tenacity of the coral-like TiO_2 on the FTO substrate after annealing at 450 ˚C for 1 h. Under illumination, the resulting photoinduced charge accumulation at annealed coral-like TiO_2 is believed to be the reason for the significantly increased photocurrent.

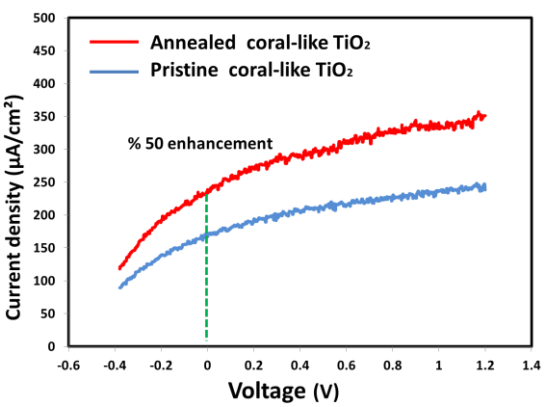

Figure 6. J-V curves of the pristine and annealed coral-like TiO_2 photoanodes with 50% enhencement under illumination versus Ag/AgCl as reference.

Conclusions

In conclusion, we have synthesized rutile coral-like TiO_2 as effective photoanode with high effective surface area originating from its shape for water splitting and generation of H_2 under illumination. Annealing process at 450 ˚C led to an improvement in photoelectrochemical properties of the obtained coral-like TiO_2 and enhancement of current density of about %50.

Acknowledgements

The authors would like to thank Research Council of the Tarbiat Modares University for financial supports.

References

[1]A. Kudo, Y. Miseki, Heterogeneous photocatalyst materials for water splitting, Chemical Society Reviews, 38 (2009) 253-278.

[2] J. Ye, Z. Zou, A. Matsushita, A novel series of water splitting photocatalysts NiM_2O_6 (M= Nb, Ta) active under visible light, International Journal of Hydrogen Energy, 28 (2003) 651-655.

[3] J. Xing, W.Q. Fang, H.J. Zhao, H.G. Yang, Inorganic photocatalysts for overall water splitting, Chemistry–An Asian Journal, 7 (2012) 642-657.

[4] M. Zirak, M. Ebrahimi, M. Zhao, O. Moradlou, M. Samadi, A. Bayat, H.-L. Zhang, A. Moshfegh, Fabrication and surface stochastic analysis of enhanced photoelectrochemical activity of a tuneable MoS_2–CdS thin film heterojunction, RSC Advances, 6 (2016) 16711-16719.

[5] A. Fujishima, Electrochemical photolysis of water at a semiconductor electrode, nature, 238 (1972) 37-38.

[6] B. O'regan, M. Grfitzeli, A low-cost, high-efficiency solar cell based on dye-sensitized, nature, 353 (1991) 737-740.

[7] S. Cao, K.L. Yeung, J.K. Kwan, P.M. To, C. Samuel, An investigation of the performance of catalytic aerogel filters, Applied Catalysis B: Environmental, 86 (2009) 127-136.

[8] Y.-C. Chou, Y. Ku, Preparation of high-aspect-ratio TiO_2 nanotube arrays for the photocatalytic reduction of NO in air streams, Chemical engineering journal, 225 (2013) 734-743.

[9] Y. Gao, P. Fang, F. Chen, Y. Liu, Z. Liu, D. Wang, Y. Dai, Enhancement of stability of N-doped TiO_2 photocatalysts with Ag loading, Applied Surface Science, 265 (2013) 796-801.

[10] Y. Dong, D. Tang, C. Li, Photocatalytic oxidation of methyl orange in water phase by immobilized TiO_2-carbon nanotube nanocomposite photocatalyst, Applied Surface Science, 296 (2014) 1-7.

[11] D. Dambournet, I. Belharouak, K. Amine, Tailored Preparation Methods of TiO_2 Anatase, Rutile, Brookite: Mechanism of Formation and Electrochemical Properties, Chemistry of materials, 22 (2009) 1173-1179.

[12] D. Reyes-Coronado, G. Rodríguez-Gattorno, M. Espinosa-Pesqueira, C. Cab, R.d. de Coss, G. Oskam, Phase-pure TiO_2 nanoparticles: anatase, brookite and rutile, Nanotechnology, 19 (2008) 145605.

[13] A.S. Attar, Z. Hassani, Fabrication and Growth Mechanism of Single-crystalline Rutile TiO_2 Nanowires by Liquid-phase Deposition Process in a Porous Alumina Template, Journal of Materials Science & Technology, 31 (2015) 828-833.

[14] J. Yan, G. Wu, N. Guan, L. Li, Z. Li, X. Cao, Understanding the effect of surface/bulk defects on the photocatalytic activity of TiO_2: anatase versus rutile, Physical Chemistry Chemical Physics, 15 (2013) 10978-10988.

[15] L. Miao, P. Jin, K. Kaneko, A. Terai, N. Nabatova-Gabain, S. Tanemura, Preparation and characterization of polycrystalline anatase and rutile TiO_2 thin films by rf magnetron sputtering, Applied Surface Science, 212 (2003) 255-263.

[16] Y. Yamamoto, Y. Matsumoto, H. Koinuma, Homo-epitaxial growth of rutile TiO_2 film on step and terrace structured substrate, Applied surface science, 238 (2004) 189-192.

[17] R. Long, Understanding the Electronic Structures of Graphene Quantum Dot Physisorption and Chemisorption onto the TiO_2 (110) Surface: A First-Principles Calculation, ChemPhysChem, 14 (2013) 579-582.

[18] Y. Yu, J. Ren, M. Meng, Photocatalytic hydrogen evolution on graphene quantum dots anchored TiO_2 nanotubes-array, International Journal of Hydrogen Energy, 38 (2013) 12266-12272.